

1 **RaDeCC Reader: Fast, accurate and automated data processing for Radium**

2 **Delayed Coincidence Counting systems**

3 **Sean Selzer^{1*}, Amber L. Annett², William B. Homoky^{1,3}**

4 1. Department of Earth Sciences, University of Oxford, South Parks Road, Oxford, OX1 3AN, UK

5 2. Ocean and Earth Science, University of Southampton, Waterfront Campus, National Oceanography
6 Centre, European Way, Southampton, SO14 3ZH, UK

7 3. Present address: School of Earth and Environment, University of Leeds, Leeds, LS2 9JT, UK

8 [*sean.selzer@earth.ox.ac.uk](mailto:sean.selzer@earth.ox.ac.uk)

9

10 **Code Availability:**

11 RaDeCC Reader program and supporting files can be found on GitHub

12 Github Repository: (https://github.com/oxradreader/RaDeCC_Reader/releases)

13

14 **Authorship Statement:**

15 S.S. conceived and wrote the RaDeCC Reader program and A.L.A. and W.B.H. contributed to
16 its design, testing and implementation. A.L.A. provided real sample data files and S.S. carried
17 out the validation experiments. S.S. prepared the manuscript, with edits and contributions
18 throughout from A.L.A. and W.B.H.

19

20 **Abstract**

21 A Python program is presented to expedite the process of correcting raw data and propagating
22 the related uncertainties from Radium Delayed Coincidence Counting (RaDeCC) instruments.
23 The performance of the program was validated against an established method with real data.
24 Excellent agreement between determinations of excess radium-223, actinium-227, excess
25 radium-224, thorium-228 and radium-226 was achieved, with minor discrepancies in the

26 results attributed to logical improvements in our implementation. The RaDeCC Reader
27 program is able to process one thousand data files in only a few minutes, and thereby offer
28 distinct advantages in the processing speed combined with reliable accuracy of data processing
29 implementations.

30

31 **Keywords:** Data Processing; Software Engineering; Data Assimilation; Environmental
32 Science; Hydrogeology;

33

34 **1. Introduction**

35 Radium is a valuable tracer for environmental geochemistry due to the conservative nature of
36 radium in seawater and the predictable rates of decay of its isotopes. Disequilibria between
37 these isotopes can allow the quantification of rates of exchange between natural reservoirs
38 (Cochran, 1982). The development of Radium Delayed Coincidence Counting (RaDeCC)
39 systems has made radium-based studies in aqueous environments more feasible (Moore and
40 Arnold, 1996). For example, radium isotopes are increasingly used to trace, quantify and
41 advance understanding of many fundamental ocean processes in coastal (Moore, 2000;
42 Tamborski et al., 2020), shelf sea (Hendry et al., 2019), open ocean surface (Charette et al.,
43 2007) and deep water settings (Kipp et al., 2018).

44 To measure the activities of radium-223 and radium-224 in aqueous environments, sample
45 water is commonly pumped through manganese oxide impregnated acrylic or polyethylene
46 fibres (Moore, 1976). These fibres extract radium, its parent isotopes thorium and actinium,
47 and other species with high affinity for MnO_2 , from the water via binding to the MnO_2
48 functional groups present on the fibres. The precise activities of radium isotopes on these fibres
49 can be determined by counting their daughter isotopes radon and polonium using a scintillation

50 counting technique that is optimally performed by the RaDeCC apparatus
51 (<https://www.radecc.com>) (Moore and Arnold, 1996).

52 The RaDeCC system of delayed coincidence counting was originally devised by Giffin *et al.*,
53 (1963) and forms the basis of the RaDeCC apparatus devised by Moore and Arnold, (1996).

54 The RaDeCC apparatus measures the activities of radon isotopes – the nuclides produced from
55 radium decay - emanating from sample fibres over the course of a counting period, herein
56 termed “read”. The flow of helium through a closed loop carries this radon between the sample
57 fibre container and the scintillation cell. Radon decay in the scintillation cell produces an alpha
58 particle which is detected, generating a signal which is routed to three channels: total counts,
59 radon-219 and radon-220. The total counts channel records a count when any signal is received.

60 In the radon-219 and radon-220 channels the system looks for a second count, corresponding
61 to the subsequent decay of daughters polonium-215 and polonium-216 (respectively) after a
62 short delay for the signal to stabilise: 0.01 ms for the radon-219 channel and 5.61 ms for the
63 radon-220 channel (Moore and Cai, 2013). After these delays a gate is opened in each channel
64 (5.6 ms and 600 ms for radon-219 and radon-220, respectively; Moore and Arnold, 1996) in
65 which an additional signal of alpha decay is required in order to register a count. During a read
66 the RaDeCC software logs the counts and accumulated counts per minute for each channel at
67 regular user-defined intervals to a text file.

68 Factors that need to be corrected for in the raw output include: interference between the detector
69 channels for radon-219 and -220 and chance coincidence events; the counting efficiency and
70 background (blank) of each detector; decay that occurred between sampling and measurement;
71 rescaling sample activities to their original sample volumes (Giffin *et al.*, 1963; Moore and
72 Arnold, 1996). The expressions used to propagate uncertainties associated with these
73 corrections were derived by Garcia-Solsona *et al.*, (2008).

74

75 The amount of radium parent isotope on the MnO₂ coated fibres determines the rate of
76 production of the radon isotope daughter, and therefore the activity sustained in the flow of
77 helium through a closed loop between sample and the RaDeCC system. The decay of actinium
78 and thorium on the fibres supplements the amount of ‘excess’ radium-223 and radium-224 that
79 is initially present (creating supported activity) leading to the activities of radon-219 and radon-
80 220 initially measured by the RaDeCC system. These supported activities must be accounted
81 for to accurately determine the excess, or unsupported, activities of radium-223 and radium-
82 224. Finally, there is the ingrowth of radon-222 from its long-lived parent isotope, radium-226,
83 recorded by the total channel. Determining the rate of radon-222 ingrowth can be used to
84 estimate the activity of radium-226 (Geibert et al., 2013).

85 To perform the necessary raw data correction and uncertainty propagation calculations, many
86 workers construct large Excel spread sheets and individually import their saved read file
87 outputs from RaDeCC apparatus. Although this process allows a very granular view of the raw
88 data and can serve its purpose well, it remains time intensive and large sets of data are
89 susceptible to user-error. A faster, user-defined automation that preserves details of the
90 calculation processes could therefore offer significant improvements to data processing speed
91 and the reliability of outputs. Herein, we present our approach to expedite the process of
92 correcting raw data and propagating the related uncertainties from Radium Delayed
93 Coincidence Counting (RaDeCC) instruments using a newly designed program, RaDeCC
94 Reader. We prove the validity of our new method by comparing results obtained with RaDeCC
95 Reader to those we obtained by a previously established method using real data collected from
96 karstic spring-, coastal- and open-ocean water samples.

97

98 **2. Theory**

99 **2.1 Calculation of excess radium-223 and radium-224 activities**

100 To convert raw decay counting statistics into the activity of radium-223 or radium-224 of a
 101 sample, a number of factors must be considered and corrected for. A table of variables and their
 102 units is included for reference (Table 1). Uncertainties in the raw counts must also be
 103 propagated through each of these corrections to determine uncertainties in final calculated
 104 activities.

105 An erroneously registered count due to chance coincidence events ($Y\ CC$, in cpm) is the first
 106 correction to be made. An erroneous count can be made when a decay event that is unrelated
 107 to the isotope of interest occurs while the detector-gate for that isotope's channel is open. These
 108 can originate from the background activity in the detectors or the decay of radon-222 while the
 109 219 or 220 channels are open. The counts per minute (cpm) attributed to chance coincidence
 110 events are subtracted from the count rate in the relevant channel. Expressions to calculate the
 111 fraction of chance coincidence events in each channel (Equations 1,2) were derived by Giffin
 112 *et al.* (1963) and were included by Garcia-Solsona *et al.* (2008), where $cpm\ total$, $cpm219$ and
 113 $cpm220$ are the counts per minute in the total, 220 and 219 counting channels respectively.

$$114 \quad Y\ 220\ CC = \frac{(cpm\ total - cpm220 - cpm219)^2 \times 0.01}{1 - [(cpm\ total - cpm220 - cpm219) \times 0.01]} \quad (1)$$

$$115 \quad Y\ 219\ CC = \frac{(cpm\ total - corr220 - cpm219)^2 \times 0.000093}{1 - [(cpm\ total - corr220 - cpm219) \times 0.000093]} \quad (2)$$

116 These chance coincidence events are then subtracted from the counts per minute in the relevant
 117 channel to determine the coincidence corrected counts ($corr220$, $corr219$).

$$118 \quad corr220 = cpm220 - Y\ 220\ CC \quad (3)$$

$$119 \quad corr219 = cpm219 - Y\ 219\ CC \quad (4)$$

120 In certain circumstances the decays associated with radon-219 can be erroneously registered in
 121 the 220-channel. This can happen if two atoms of radon-219 decay within the time that the 220
 122 channel is open. Radon-220 can also cause interference in the radon-219 channel since the gate
 123 for this channel is open for enough time that 2.55% of radon-220 decay events occur while the

124 gate is open. Expressions to account for these cross-channel interferences were devised by
 125 Giffin et al. (1963) and adapted by Moore and Arnold (1996).

$$126 \quad final\ 220 = corr220 - \frac{(1.6 \times corr219)^2 \times 0.01}{1 + [(1.6 \times corr219) \times 0.01]} \quad (5)$$

$$127 \quad final\ 219 = corr219 - (corr220 \times 0.0255) \quad (6)$$

128

129 In addition, background measurements may be run with MnO₂-coated fibres that were not used
 130 for sampling, assessing any counts due to contamination on fibre or within the RaDeCC
 131 apparatus itself, although the need for a background correction varies with sample type and
 132 application. Where required, the background count rate (in cpm) in each channel is averaged
 133 over multiple reads for each detector. The averaged background count rate from the applicable
 134 detector and channel is then subtracted from *final220* and *final219* before detector efficiencies
 135 are accounted for (*bkgcorr224*, *bkgcorr223* respectively; Equations 7,8).

$$136 \quad bkgcorr224 = final220 - Average_bkg_220 \quad (7)$$

$$137 \quad bkgcorr223 = final219 - Average_bkg_219 \quad (8)$$

138

139

140 The detection efficiencies, *E219* and *E220*, are evaluated by measuring the activities of
 141 standards with a known amount of radium-223 or radium-224 adsorbed to their fibres and
 142 comparing these measured activities (in cpm) to their known activities (in dpm) after
 143 corrections for decay since manufacture (Equations 9,10). These standards are made by
 144 adsorbing known activities of thorium-232 or actinium-227 in secular equilibrium with their
 145 daughter isotopes, radium-224 and radium-223 respectively.

$$146 \quad E220 = \frac{final220\ (standard)}{thorium-232} \quad (9)$$

$$147 \quad E219 = \frac{final219\ (standard)}{actinium-227} \quad (10)$$

148

149 Alternatively $E219$ can be determined from $E220$ using equations 11 and 12 (Moore and Cai,
 150 2013).

$$151 \quad \text{Ratio}_{E219/E220} = \frac{P_{219} \times (1 - L_{219})}{P_{220} \times (1 - L_{220})} \quad (11)$$

$$152 \quad E219 = E220 \times \text{Ratio}_{E219/E220} \quad (12)$$

153

154 In which $E220$ is the 220-channel system efficiency, P is the probability of the radon isotope
 155 decaying in the counting cell and L is the fractional loss due to delay and window settings.
 156 Fraction loss (L) will depend on the default RaDeCC apparatus time constants or those set by
 157 the operator as described by Moore and Cai (2013). The ratio $E219/E220$ for the RaDeCC with
 158 default settings and normal configuration is 0.91 (Moore and Cai, 2013).

159

160 The counts per minute due to radon-219 and radon-220 are converted to disintegrations per
 161 minute (dpm) by dividing $final220$ or $final219$ by the detection efficiency of the channel, ($E219$
 162 or $E220$, respectively; Equations 13,14) (Giffin et al., 1963; Moore and Arnold, 1996).

$$163 \quad dpm224 = \frac{bkgcorr224}{E220} \quad (13)$$

$$164 \quad dpm223 = \frac{bkgcorr223}{E219} \quad (14)$$

165

166 Finally, the dpm values are divided by the sample *volume* (or mass) to produce the volume-
 167 corrected radium-223 ($vdpm223$) and radium-224 ($vdpm224$) sample activities (both in dpm m⁻³)
 168 for each read (Equations 15,16).

$$169 \quad vdpm224 = \frac{dpm224}{Volume} \times 1000 \quad (15)$$

$$170 \quad vdpm223 = \frac{dpm223}{Volume} \times 1000 \quad (16)$$

171 To obtain the excess radium-224 and radium-223 activities of the samples at the time of
 172 sampling, two further factors must be accounted for: decay of the isotope between sampling

173 and measurement and any activity supported by the parent isotope. The respective parent or
 174 supporting isotopes of radium-223 and radium-224 are actinium-227 and thorium-228.
 175 In order to distinguish the activities of parent and daughter isotopes, each sample must be
 176 analysed multiple times at different intervals relative to the time of collection. The 1st interval
 177 read, performed as soon after sampling as possible, is a measurement of radium-223 and
 178 radium-224 activity, this will be a combination of excess and supported activities. A 2nd
 179 interval, 7-10 days after sampling, can provide a more accurate radium-223 activity due to
 180 reduced interference from radium-224 and radon-220 decay (Moore, 2008), and is essential in
 181 instances where the 220/219 count rate is greater than 10, or greater than 4 and the 220 channel
 182 exceeds 5 cpm (Diego Feliu et al. 2020). Eventually, >99% of measured radium-224 and
 183 radium-223 activities will be supported by their parent isotopes. This occurs after 25 days for
 184 radium-224 and after 80 days for radium-223, and dictates the timing of 3rd and 4th intervals.
 185 In effect, 3rd and 4th interval reads provide an indirect measurement of these parent isotope
 186 activities, thorium-228 and actinium-227 respectively.

$$187 \quad {}_{xS}^{223}Ra = \frac{{}_{i}^{223}Ra - {}_{S}^{223}Ra}{e^{-\lambda_{223}t}} \quad (17)$$

$$188 \quad {}_{xS}^{224}Ra = \frac{{}_{i}^{224}Ra - {}_{S}^{224}Ra}{e^{-\lambda_{224}t}} \quad (18)$$

189 Excess radium-224 and excess radium-223 at the time of sampling is then calculated via
 190 equations 17 and 18, where ${}_{i}^{223}Ra$ and ${}_{i}^{224}Ra$ are the radium-223 activity of the 1st or 2nd
 191 interval read and the radium-224 activity of the 1st interval read, ${}_{S}^{223}Ra$ the activity supported
 192 by actinium-227 decay (4th interval) and ${}_{S}^{224}Ra$ the radium-224 activity supported by thorium-
 193 228 decay (3rd interval). The time between sampling (in days) and the first measurement of
 194 each isotope is denoted by t and the respective decay constants of radium-223 and radium-224
 195 by λ_{223} and λ_{224} . For all calculations, including detector efficiencies, error propagation
 196 follows the equations presented in Garcia-Solsona et al. (2008).

197 **2.2 Calculation of radium-226 activity**

198 The activity of long-lived radium-226 is measured indirectly via the rate of ingrowth of its
199 decay product, radon-222. The half-life of radon-222 is 3.8 days, so as radium-226 in the
200 sample decays over the course of a read, radon-222 accumulates in the system. This
201 accumulation is seen in the total channel, with counts in the total channel increasing throughout
202 the read in proportion to the radium-226 activity of the sample (Geibert et al. 2013). The *slope*
203 *of cpm total* versus time during a run thus provides a measure of the radium-226 activity of the
204 sample, based on the conversion factor ‘*m*’, which has a theoretical value of $1.80 \pm 0.07 \cdot 10^{-4}$
205 min^{-1} (Diego-Feliu et al. 2020).

206 Each RaDeCC detector must also be calibrated by measuring a standard with known radium-
207 226 activity, calculated as for *E220* in equation 7. Volume-corrected radium-226 activity of
208 the sample (*vdpm226*, in dpm/m^3) is then calculated using equation 20, where ‘*vdpm226initial*’
209 is the initial volume corrected radium-226 activity (in cpm/m^3 ; equation 19) and ‘*E226*’ is the
210 efficiency of system in determining radium-226 activity. This method was devised by Geibert
211 et al., (2013) and modified by Diego-Feliu et al., (2020).

$$212 \quad v\text{dpm}226_{\text{initial}} = \frac{\text{slope of cpm total}}{m} \div \text{Volume} \times 1000 \quad (19)$$

$$213 \quad v\text{dpm}226 = \frac{v\text{dpm}226_{\text{initial}}}{E226} \quad (20)$$

214

215 **3. Implementation: The RaDeCC Reader Program**

216 The RaDeCC Reader program is a collection of python scripts that quickly processes RaDeCC
217 output files. The program works from a single folder containing all read files including those
218 of standards and backgrounds (or blanks), sample log sheets and a small amount of user input
219 via a graphical user interface (GUI; Figure 1). From this folder, it creates an organised directory
220 of read files, a table of calculated detector efficiencies with propagated uncertainties and a table
221 of corrected excess radium-223, excess radium-224, thorium-228, actinium-227 and radium-

222 226 activities (in dpm/m³) (Figure 2). The tabulated outputs also detail each correction and its
223 propagated uncertainty for each read of each sample. Additional transparency is provided by
224 plots of counts-per-minute vs. time for the 219, 220 and total channels, produced for each read
225 (Figure 3) as well as plots depicting any anomalous spikes that have been automatically
226 removed. Data quality warnings and errors are also flagged alongside calculated results in
227 output tables as outlined in Section 3.2.2.

228 **3.1 Essential information for the program**

229 The RaDeCC Reader program receives information in three ways: text files output by the
230 RaDeCC apparatus, the sampling log-sheet and the graphical user interface (GUI). Information
231 entered into the GUI entry fields are used to aid the program in file-handling and provide
232 standard and instrument specific parameters required for the data corrections and uncertainty
233 propagations. Once completed these GUI entries can be saved by the user and reloaded for
234 subsequent runs of the program.

235 **3.1.1 Directories**

236 To start, the user sets up the following folder and contents:

237 *C:/.../Main_folder/Read_files_and_logsheets/*

238 *C:/.../Main_folder/RaDeCC_Reader_Scripts/*

239 The first entry fields in the GUI are the input and output directories (Figure 1a) and the logsheet.
240 The input directory is where the program will find all the input read files and the logsheet. The
241 output directory is where the program will place the organised read files, the logsheet file and
242 output files.

243 **3.1.2 Logsheets: Linear and Branched sample sets**

244 Logsheets form the basis of the eventual output files, in which all the metadata contained within
245 a logsheet will be included. A logsheet must contain information that is essential to data
246 correction calculations: sample names, sample volumes and mid-point sampling times; as well

247 as any sub-sample names (for herein so-called ‘branched’ datasets) if applicable. There should
248 be a column displaying each of these variables in a logsheet. Any additional information
249 contained in a logsheet (e.g. the latitude, longitude and depth of individual samples) is
250 preserved in the output files and will not interfere with the calculations but may prove useful
251 for later analysis. An example logsheet file is included in the Supplementary Information. The
252 date format convention for read files and the logsheet must be consistent and can be indicated
253 via a tickbox in the GUI.

254 Data outputs can be organised differently to assist the user. How data outputs will be organised
255 depends on whether or not the user indicates a sample set includes sub-samples. Herein sample
256 sets that do not contain sub-samples (e.g. multiple locations sampled once, or time series at a
257 single location) are termed ‘linear’. Sample sets with sub-samples (e.g. multiple locations each
258 sampled at multiple times, or a series of depth profiles) are termed ‘branched’. In the case of a
259 sample set where some samples have sub-samples, this could be processed using the branched
260 setting. In this case, samples without subsamples would be seen as samples with one subsample
261 each. The distinction between linear and branched can be indicated via a tickbox in the GUI.

262 **3.1.3 File naming and identifiers**

263 In order to acquire raw data, the program requires the text files generated by the RaDeCC
264 systems for sample, standard and (if required) background reads. The formatting of these
265 filenames needs to be consistent and must include information on the sample (and sub-sample)
266 name and the detector used. For example, ‘1-StnX001-A001-010220-det1.txt’, contains the
267 sample name ‘StnX001’, subsample name ‘A001’ and the detector name ‘det1’. The number
268 ‘1’ at the start of the file name designates the read interval (e.g. 1 for radium-224
269 quantification), although this is recorded by the program it is not used in excess calculations.
270 Instead, the program assigns a read interval automatically by calculating the elapsed time
271 between sampling and RaDeCC analysis. It is important to note that sample and sub-sample

272 names must be distinct from each other, no sample name should contain another sample name
273 within it (StnX1 and StnX10, for example). Once the first panel of entries is completed in the
274 GUI (Figure 1a), these entries are checked by the program, and if verified, the user can proceed
275 to the second panel in the GUI to assign details of the standards and backgrounds.

276

277 **3.1.4 Information on detectors, standards and backgrounds**

278 Upon verified completion of the first panel of entries in the GUI (Figure 1a), a second panel
279 will appear requesting inputs for individual detectors (names, *E219/E220* ratios, radium-226
280 slope calibration values and radium-226 system efficiency values) and details specific to
281 individual standards (names, dates of manufacture and initial activity) (Figure 1b). Only an
282 identifying name is requested for background runs. If background measurements are not
283 required then the ‘No. of Background Standards’ field can be set to ‘0’ in panel 1 of the GUI
284 (Figure 1a). These inputs are all required for the calculation of detector efficiencies and the
285 resulting corrections to the raw data.

286 **3.1.5 Assigning variables**

287 The final GUI entries are the titles of log-sheet columns containing sample name, sub-sample
288 name, sample volume, sample volume error, sampling date and sampling time. These column
289 titles should not contain spaces and must be selected via the drop-down lists that appear in the
290 second panel of the GUI after a log-sheet file is selected in the first (Figure 1b).

291 Once these details are completed and verified, the user can then proceed to run the RaDeCC
292 Reader. A step-by-step explanation of information input and program setup is also provided in
293 the *Instructions.md* or *Instructions.txt* files in the GitHub repository along with example data
294 to check that the program is functioning properly.

295 **3.2 How it works**

296 **3.2.1 Data, directories and detector efficiencies**

297 Upon clicking the 'Run RaDeCC Reader' button, the directory building function will create an
298 organised directory of read and logsheet files using input from the GUI as well as sample and
299 sub-sample names in the logsheet.

300 The `directory_filler` function will then use each folder/sub-folder name as a search criteria and
301 search through the main folder of reads for files that match each folder name and then
302 subsample. When a match occurs, the file is copied to the folder it was matched with. Any files
303 not matching sample/sub-sample folder names or standard or background folder names will be
304 copied to the miscellaneous (*misc.*) folder.

305 Once the directory is built and populated with reads, a dataframe of detector efficiencies is
306 produced. The efficiencies calculation function searches through the appropriate standard and
307 background subfolders for each detector specified by the user in the GUI. The program creates
308 a dataframe of corrected reads for each standard with the appropriate channel efficiency for
309 each read calculated as well as a dataframe of background reads. These offer the user a more
310 granular view of read results when validating the average efficiencies displayed in the summary
311 efficiencies dataframe. These four dataframes are automatically exported as .csv files. The
312 detector efficiency of the 219-channel for each detector is calculated using the actinium-227
313 standard as well as the method devised by Moore and Cai (2013), based on system volume and
314 220-channel efficiency using the thorium-232 standard. In parallel, the two separate 219-
315 channel efficiencies are used to calculate two separate final corrected radium-223 values. Use
316 of radium-223 values based on the Moore and Cai (2013) method requires verification of an
317 E_{219}/E_{220} ratio (Section 3.1.4): the Reader includes the value determined by Moore and Cai
318 for the standard RaDeCC configuration as a default.

319 The program uses the sample name (and sub-sample name) in each row of the logsheet as
320 search criteria, finding the corresponding read files to scan. Using the data scanned from the
321 read files the program performs the appropriate corrections and related propagation of

322 uncertainties. For each read, these new corrected values along with their uncertainties are
323 combined with the sample's corresponding metadata from the logsheet and entered as a new
324 row in the read results dataframe.

325 **3.2.2 First level corrections**

326 Every read file for each sample/sub-sample is scanned, the interval logged data is extracted
327 from the text file, and the first level of corrections are performed (Garcia-Solsona et al., 2008).

328 These include:

- 329 - Chance coincidence counts per minute in the 219 and 220 channels (*Y 219 CC, Y 220 CC*)
- 330 - Corrections for 220 interference in the 219 channel (to give *final219*)
- 331 - Corrections for 219 interference in the 220 channel (to give *final220*)
- 332 - Total counts corrected for counts due to 219 or 220 (to give *corr total*)

333 As the program scans through a read, each interval is evaluated using the guidelines outlined
334 by Diego-Feliu et al., (2020) for the measurement and quantification of radium-223 and
335 radium-224 (Figure 4). For each read, the program records the percentage of intervals for which
336 quantification of radium-223 or radium-224 is not recommended and logs these percentages in
337 an error column of the read results dataframe. This allows the user to quickly establish whether
338 an anomalous result might be due to cross-talk or other interferences. The scanning of read
339 files is not obstructed by files with lines enclosed by quotation marks or extra lines added by a
340 pause function.

341 **Spike removal:** If the number of counts in either the total, 219- or 220-channel during one
342 time interval is higher than the next interval by more than the '*Spike sensitivity*' constant the
343 program removes this time interval as it is considered to contain a counting anomaly - likely
344 due to a spike in the electrical supply to the RaDeCC apparatus. If an anomaly is removed, the
345 value of the anomaly is recorded in the *Spike_Value* column of the results dataframe. The
346 calculated counts per minute values of each interval are then averaged over the whole read.

347 The '*Spike sensitivity*' constant is set at 10^6 counts by default, meaning that spike removal is
348 inactive, but may be activated via a change in the '*Spike sensitivity*' constant value by the user
349 to allow for higher or lower sample activities.

350 **Radium-226 estimates from radon-222 ingrowth and Raw Data Plots:** The rate of radon-
351 222 ingrowth seen in the Total channel (*cpm total*) is calculated in order to estimate the activity
352 of radium-226 in the sample. The equilibration time variable (0 minutes as default) allows the
353 user to set the time required for the radon-222 activity throughout the RaDeCC circuit to
354 accumulate sufficiently to be detectable in the total channel. The time interval is set by the user
355 in the GUI prior to initiating a read and is the number of minutes between the software logging
356 each line of the output file (Figure 1a). The time interval is used by the RaDeCC Reader
357 program here to decide how many lines to miss at the start of the read file before calculating
358 radon-222 ingrowth and therefore the radium-226 activity estimate. A plot of read-time vs.
359 total counts per minute (*cpm total*), 219 channel counts per minute (*cpm219*) and 220 channel
360 counts per minute (*cpm220*) for each read is saved in the '*Read Plots*' folder (Figure 3.). These
361 plots provide a graphical view for raw data quality assessment by the user, for instance to
362 evaluate system stability as well as the build-up of radon-222 during each read. Estimated
363 radium-226 activity will only be calculated from reads with durations >600 minutes, shorter
364 reads may be less reliable due to the short period for ingrowth of radon-222 to occur. In the
365 event of a short read, the '*Err226_short_read*' error is logged in the read results dataframe.

366 **3.2.3 Second level corrections and output**

367 After the first level of corrections is complete, generating values for *final219*, *final220* and *cpm*
368 *total* for radium-226 estimation, the read results dataframe containing these new values is
369 passed on to the second level of calculations. Second level corrections expand the read results
370 dataframe with the calculated values and propagated uncertainties as described by Garcia-
371 Solsona *et al.* (2008). Second level corrections include:

- 372 - Detector background corrections in all channels
- 373 - Corrections for detector channel efficiencies
- 374 - Corrections for sample volume, producing volume corrected activity (*vdpm*)

375 These final calculations complete the series of corrections and uncertainty propagations
376 providing disintegrations per minute per 1000 L (dpm/m³) for radium-223 and radium-224 as
377 well as an estimate of radium-226 activity (dpm/m³) for each read. These individual read results
378 are saved as a table in comma-separated-value (.csv) format before being combined to calculate
379 sample activities.

380 **3.2.4 Sample activity calculations and outputs**

381 The final stage of calculations is the combination of read-specific values calculated in the
382 results dataframe to calculate excess radium-223, excess radium-224, radium-226, actinium-
383 227 and thorium-228 activities for each sample.

384 The 2nd and 4th interval reads of each sample/sub-sample are combined using equation 13 to
385 calculate excess radium-223. For the calculation of excess radium-224, 1st and 3rd interval reads
386 are combined using equation 14. In many circumstances 1st interval reads are sufficient to
387 accurately quantify radium-223 activity, so if 2nd interval reads are unavailable, excess radium-
388 223 is calculated using 1st reads. Similarly, if 3rd reads are unavailable, excess radium-224 is
389 calculated using 4th interval reads. Actinium-227 activity is essentially the supported radium-
390 223 activity calculated for the 4th (or 3rd) interval read of a sample/sub-sample while thorium-
391 228 is the supported radium-224 activity calculated for the 3rd (or 4th) interval read of a
392 sample/sub-sample. If the results dataframe contains more than one read of a particular
393 sample/sub-sample for a given interval (1st-4th), the average activity of the relevant reads will
394 be used in the calculation. The radium-226 activity of a sample is determined by averaging the
395 radium-226 activity of reads >600 minutes in duration. Any radium-226 activities that are more
396 than one standard deviation from the mean are then removed and a new average is calculated.

397 The results of these final calculations are tabulated in a summary dataframe and exported as a
398 comma-separated value (.csv) file. Any read-interval substitutions in the calculation of excess
399 activities are logged in the error column of this summary dataframe alongside any errors raised
400 using the logic outlined by Diego-Feliu et al. (2020) for all read results used.

401 **4. Validation**

402 **4.1 Experimental Design**

403 To evaluate the performance and accuracy of the RaDeCC Reader program, the processing
404 time and corrected data outputs from real sample, standard and background determinations by
405 RaDeCC instruments were compared to those derived from a Microsoft Excel implementation
406 of the calculations outlined by Garcia-Solsona et al. (2008) and Geibert et al. (2013).

407 A total of 208 raw data files from 44 samples were used for the purpose of this evaluation.
408 Open ocean samples (106 raw data files, 19 seawater samples) were collected from 60-100
409 litres of seawater using MnO₂ impregnated fibres, during the along southwest Greenland during
410 the ICY-LAB expedition aboard RRS *Discovery* in 2017 (Hendry et al., 2019). Coastal surface
411 seawater samples (~0.5 m depth) (40 raw data files, 9 surface samples) and karstic spring-water
412 samples (62 raw data files, 16 samples) were collected offshore of the Calanques of Marseille-
413 Cassis on 27–28 March 2018 aboard the R/V Antédon II, by trace-metal clean submersible
414 pump and scuba-divers respectively (Tamborski et al., 2020).

415 The range of 219, 220 and total count rates (219: 0 - 6.3 cpm, 220: 0 – 16.8 cpm, total: 0 – 35
416 cpm) and counting times (60-4002 minutes) tested here, are realistic ranges encountered in
417 submarine aquifer and open ocean fieldwork and 35% of the maximum quantification limit of
418 the RaDeCC apparatus (Diego-Feliu et al., 2020). These samples, previously published in
419 Hendry *et al.* (2019) and Tamborski et al. (2020), were calibrated using standards prepared at
420 LEGOS, OMP (Toulouse, France) with solutions of ²²⁸Th (in equilibrium with ²³²Th) and ²²⁷Ac
421 obtained from the International Atomic Energy Agency (Monte Carlo, Monaco). Here we

422 repeat their raw data processing using our standardised Excel-based methodology and compare
423 the outputs to those obtained using the RaDeCC Reader. This approach allows any disparity in
424 results to be attributed to differences in implementation. Nine variables were compared: the
425 corrected activities of excess radium-223, actinium-227, excess radium-224, thorium-228 and
426 radium-226, and the propagated uncertainties for excess radium-223, actinium-227, excess
427 radium-224 and thorium-228.

428

429 **4.2 Results and Discussion:**

430 Implementation time of either method is certain to vary between users. For new users of the
431 RaDeCC Reader time will be needed to name and organise files and prepare logsheets. In this
432 exercise, however, the implementation of the Excel-based methodology took an experienced
433 user over 2 hours to process the outputs from standards, backgrounds and 30 samples;
434 amounting to a total of 233 raw data files. This compared to a processing time of 2 minutes to
435 perform the equivalent functions using the RaDeCC Reader, a time saving that would be
436 magnified with larger datasets or familiarity with the required file naming conventions.

437 Excellent agreement ($R^2 > 0.99$, Standard Error < 0.02) was seen for the corrected activities
438 and propagated uncertainties of excess radium-223 and excess radium-224 (Figure 5) as well
439 as actinium-227, thorium-228 (Figure 6). The small amount of variance seen, possibly due to
440 a difference in the treatment of background measurements, is an order of magnitude smaller
441 than any propagated uncertainties associated with the activities determined in this study.

442 Radium-226 activity determined by our Excel method and the RaDeCC Reader also displayed
443 very strong agreement, with greater variance than was seen for the short-lived radium isotopes
444 or their supporting isotopes ($R^2 = 0.99$, Standard Error = 0.02, Figure 6). We attribute this
445 greater variance between methods to the fact that radium-226 activities determined by RaDeCC
446 apparatus are inherently less precise than those determined for excess radium-223, actinium-

447 227, excess radium-224 and thorium-228. The activity of radium-226 is measured via the
448 ingrowth of its daughter-isotope radon-222 and therefore the slope of the activity in the total
449 channel with time. Many workers may choose not to include a portion of measurements at the
450 start of a read to allow for the partial pressure of radon-222 in the system to accumulate above
451 background. This equilibrium time may not be applied uniformly, whereas the RaDeCC
452 Reader's user defined equilibration time is applied to all reads consistently. The slope in total
453 activity with time is also sensitive to system leaks as well as the length of time a sample is
454 measured for, particularly for samples with low activity, and therefore should be evaluated
455 separately for samples with markedly different total activities.

456 **5. Conclusions**

457 We have developed a program that simplifies and expedites the process of correcting raw
458 RaDeCC data, propagating related uncertainties and calculating the activities of excess radium-
459 223, actinium-227, excess radium-224, thorium-228 and radium-226. With a logsheet and read
460 file names in the required format, the RaDeCC Reader program is capable of processing a
461 substantial real data set in a matter of minutes, and is therefore able to save users considerable
462 time and effort in data processing when compared to previous and widely used Excel-based
463 methodologies. By letting users evaluate their sampling methods and analytical performance
464 more efficiently, the RaDeCC Reader has potential to enhance experimental design, for
465 example, during maritime research expeditions. RaDeCC Reader maintained the accuracy of
466 results attributed to previous methods, and preserved transparency of data processing by
467 displaying the values of each stage of calculation, providing a view of the original raw data via
468 saved plots and flagging results with data quality warnings. We attribute minor discrepancies
469 in calculated excess radium-223, actinium-227, excess radium-224 and thorium-228 activities
470 between methods to a difference in background treatment by the RaDeCC Reader's
471 implementation. This provided no significant changes to the results from samples used in our

472 test, however the implementation used by RaDeCC Reader mitigated the risk of greater
473 inaccuracies that might have arisen from raw data files containing larger or more frequent
474 counting anomalies.

475 **Acknowledgments:**

476 The authors gratefully acknowledge support from the UK's Natural Environment Research Council
477 who funded S.S. through the Environmental Research Doctoral Training Partnership with University
478 of Oxford, and A.L.A. and W.B.H. through Independent Research Fellowships (NE/P017630/1 and
479 NE/K009532/1). We would like to thank J. Tamborski and P. van Beek who shared their RaDeCC
480 output and sample data to validate the RaDeCC Reader across a wider range of environmental
481 activities.

482 **Computer Code Availability:**

483 RaDeCC Reader, developed by Sean Selzer, Department of Earth Sciences, South Parks Rd,
484 OX1 3AN, Oxford (01865 272000, sean.selzer@earth.ox.ac.uk). First available in 2019.

485 Hardware Requirements: 2 x 64-bit 2.8 GHz 8.00 GT/s CPUs, 32 GB RAM (or 16 GB of 1600
486 MHz DDR3 RAM), 300 GB Storage.

487 Written in Python 3.6, RaDeCC Reader (179 KB) is available on GitHub
488 (https://github.com/oxradreader/RaDeCC_Reader)

489 **References:**

490 Charette, M.A., Gonneea, M.E., Morris, P.J., Fones, G., Planquette, H., Salter, I., Garabato,

491 A.N., 2007. Radium isotopes as tracers of iron sources fueling a Southern Ocean

492 phytoplankton bloom. *Deep Sea Res. Part II Top. Stud. Oceanogr.* 54, 1989–1998.

493 <https://doi.org/10.1016/J.DSR2.2007.06.003>

494 Cochran, J., 1982. The oceanic chemistry of the U- and Th-series nuclides, in: Ivanovich, M.,

495 Harmon, R. (Eds.), *Uranium Series Disequilibrium: Applications to Environmental*

496 Problems. Clarendon Press, Oxford, pp. 384–431.

497 Diego-Feliu, M., Rodellas, V., Alorda-Kleinglass, A., Tamborski, J., van Beek, P., Heins, L.,
498 Bruach, J.M., Arnold, R., Garcia-Orellana, J., 2020. Guidelines and Limits for the
499 Quantification of Ra Isotopes and Related Radionuclides With the Radium Delayed
500 Coincidence Counter (RaDeCC). *J. Geophys. Res. Ocean.* 125.
501 <https://doi.org/10.1029/2019JC015544>

502 Garcia-Solsona, E., Garcia-Orellana, J., Masqué, P., Dulaiova, H., 2008. Uncertainties
503 associated with ^{223}Ra and ^{224}Ra measurements in water via a Delayed Coincidence
504 Counter (RaDeCC). *Mar. Chem.* 109, 198–219.
505 <https://doi.org/10.1016/j.marchem.2007.11.006>

506 Geibert, W., Rodellas, V., Annett, A., Beek, P. van, Jordi Garcia-Orellana, Hsieh, Y. Te,
507 Masque, P., 2013. ^{226}Ra determination via the rate of ^{222}Rn ingrowth with the radium
508 delayed coincidence counter (RaDeCC). *Limnol. Oceanogr. Methods* 11, 594–603.
509 <https://doi.org/10.4319/lom.2013.11.594>

510 Giffin, C., Kaufman, A., Broecker, W., 1963. Delayed Coincidence Counter for the Assay of
511 Actinon and Thoron. *J. Geophys. Res.* 68, 1749–1757.

512 Hendry, K.R., Huvenne, V.A.I., Robinson, L.F., Annett, A., Badger, M., Jacobel, A.W., Ng, H.C.,
513 Opher, J., Pickering, R.A., Taylor, M.L., Bates, S.L., Cooper, A., Cushman, G.G., Goodwin,
514 C., Hoy, S., Rowland, G., Samperiz, A., Williams, J.A., Achterberg, E.P., Arrowsmith, C.,
515 Alexander Brearley, J., Henley, S.F., Krause, J.W., Leng, M.J., Li, T., McManus, J.F.,
516 Meredith, M.P., Perkins, R., Woodward, E.M.S., 2019. The biogeochemical impact of
517 glacial meltwater from Southwest Greenland. *Prog. Oceanogr.* 176, 102126.
518 <https://doi.org/10.1016/j.pocean.2019.102126>

519 Kipp, L.E., Sanial, V., Henderson, P.B., van Beek, P., Reyss, J.-L., Hammond, D.E., Moore,

520 W.S., Charette, M.A., 2018. Radium isotopes as tracers of hydrothermal inputs and
521 neutrally buoyant plume dynamics in the deep ocean. *Mar. Chem.* 201, 51–65.
522 <https://doi.org/10.1016/J.MARCHEM.2017.06.011>

523 Moore, W.S., 2008. Fifteen years experience in measuring ²²⁴Ra and ²²³Ra by delayed-
524 coincidence counting. *Mar. Chem.* 109, 188–197.
525 <https://doi.org/10.1016/j.marchem.2007.06.015>

526 Moore, W.S., 2000. Determining coastal mixing rates using radium isotopes. *Cont. Shelf Res.*
527 20, 1993–2007. [https://doi.org/10.1016/S0278-4343\(00\)00054-6](https://doi.org/10.1016/S0278-4343(00)00054-6)

528 Moore, W.S., 1976. Sampling ²²⁸Ra in the deep ocean. *Deep. Res. Oceanogr. Abstr.* 23,
529 647–651. [https://doi.org/10.1016/0011-7471\(76\)90007-3](https://doi.org/10.1016/0011-7471(76)90007-3)

530 Moore, W.S., Arnold, R., 1996. Measurement of ²²³Ra and ²²⁴Ra in coastal waters using a
531 delayed coincidence counter. *Measurement* 101, 1321–1329.

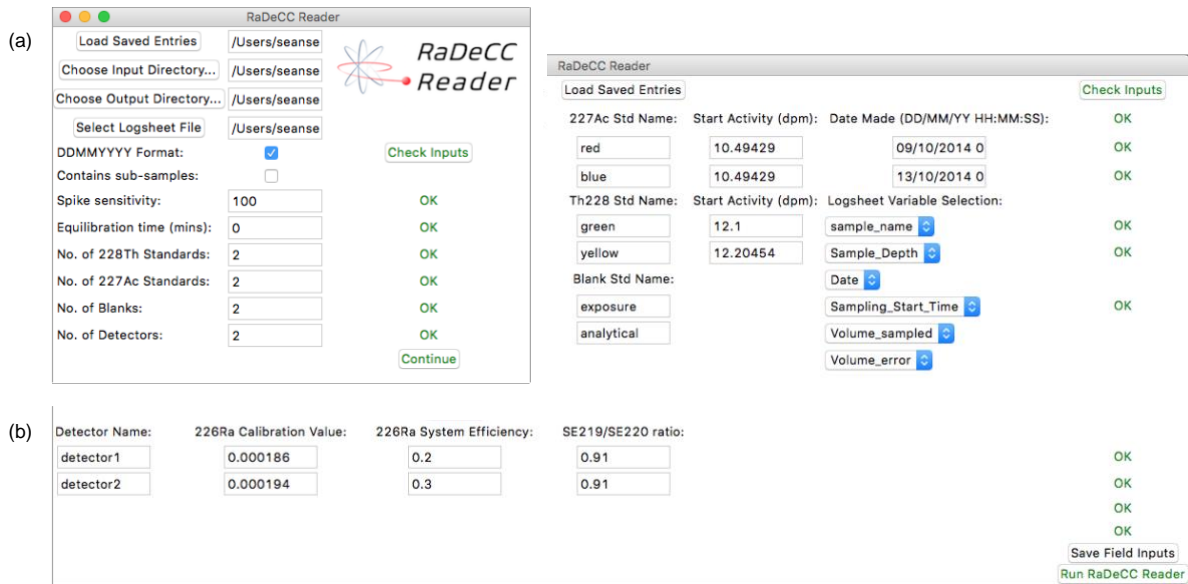
532 Moore, W.S., Cai, P., 2013. Calibration of RaDeCC systems for ²²³Ra measurements. *Mar.*
533 *Chem.* 156, 130–137. <https://doi.org/10.1016/j.marchem.2013.03.002>

534 Tamborski, J., van Beek, P., Conan, P., Pujó-Pay, M., Odobel, C., Ghiglione, J.F., Seidel, J.L.,
535 Arfib, B., Diego-Feliu, M., Garcia-Orellana, J., Szafran, A., Souhaut, M., 2020. Submarine
536 karstic springs as a source of nutrients and bioactive trace metals for the oligotrophic
537 Northwest Mediterranean Sea. *Sci. Total Environ.* 732, 1–14.
538 <https://doi.org/10.1016/j.scitotenv.2020.139106>

539

540 **Figures and Tables:**

541



542

543 **Figure 1.** Details of the Graphical User Interface (GUI) used to operate RaDeCC Reader.

544 This provides a verifiable summary of editable and necessarily user defined input parameters.

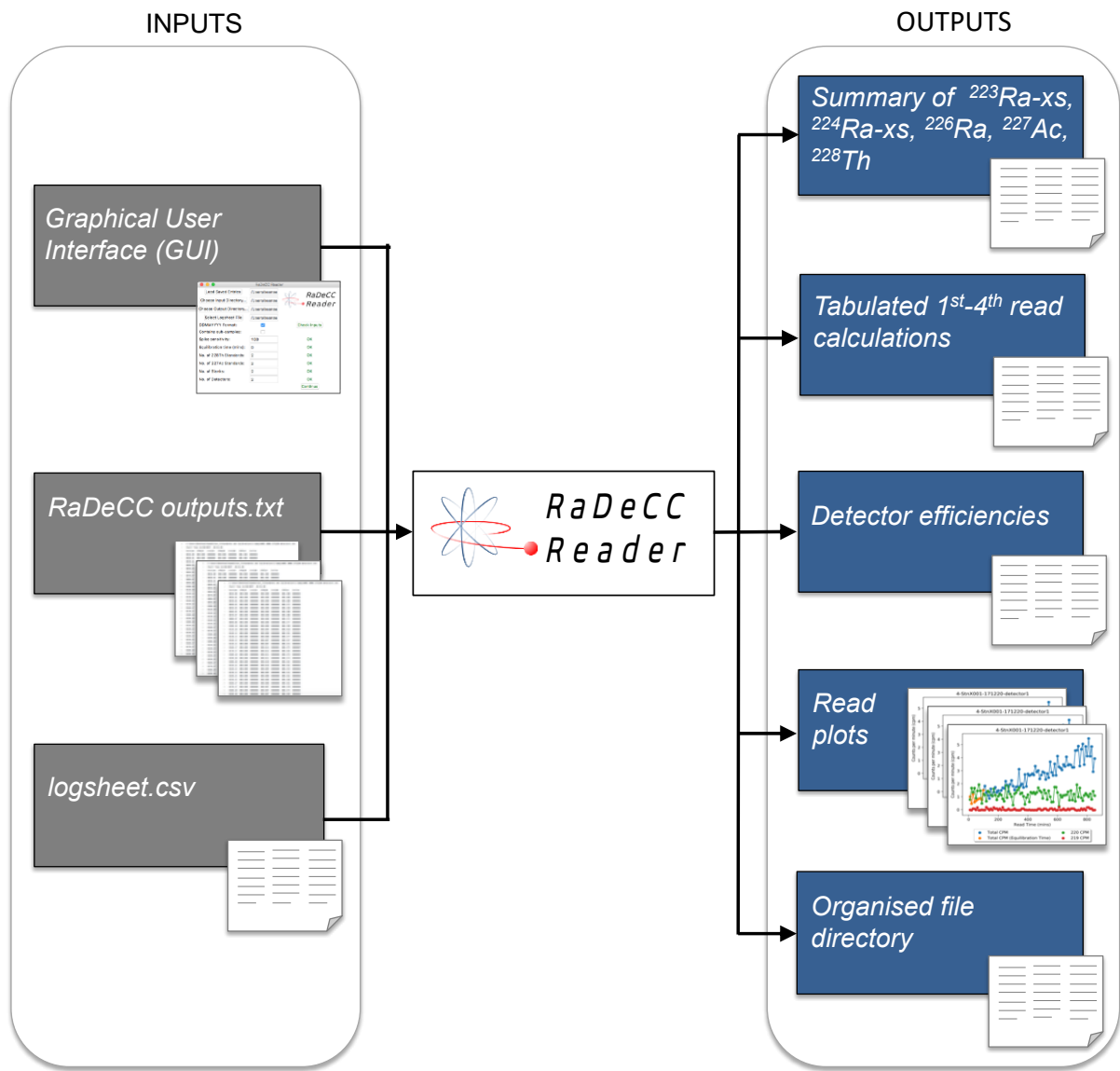
545 Including (a) input and output file directories, date and data formats, calculation preferences,

546 and the inventory of standards, backgrounds and detectors, and (b) details of individual

547 detector names and efficiencies, standard names and activities, background names, and

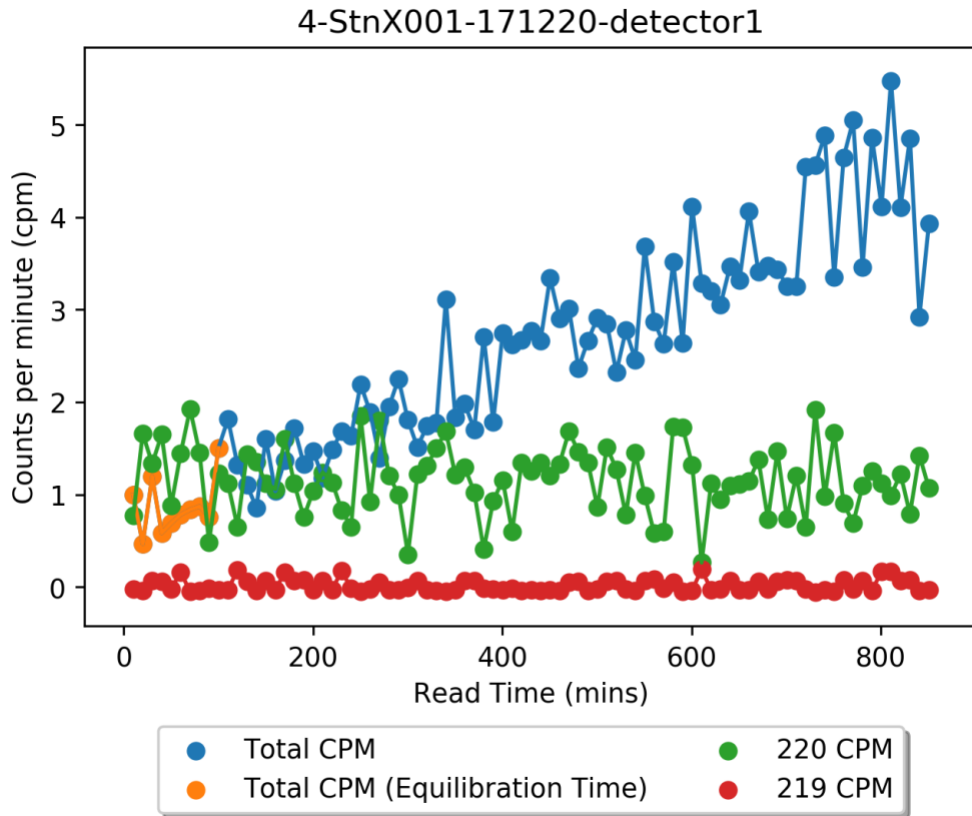
548 logsheet variables. In all fields of the GUI users may save and load previous inputs and check

549 inputs before running the RaDeCC Reader programme.



550

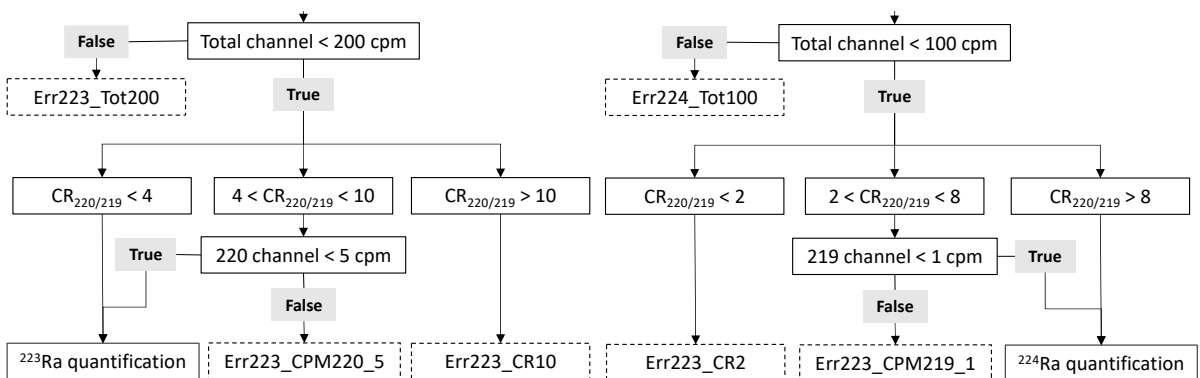
551 **Figure 2.** Summarised inputs and outputs of the RaDeCC Reader program.



552

553 **Figure 3.** Example of a read plot produced by RaDeCC Reader of counts per minute for the
 554 total, radon-219 and radon-220 channels over the course of a sample read. Spikes in counts
 555 per minute (any counts that exceeded the default ‘*Spike sensitivity*’ constant) have been
 556 removed. Counts in the total channel that are used in the estimation of radium-226 activity
 557 are shown in blue. Counts in the total channel that are ignored in the estimation of radium-
 558 226 activity during a user-defined period of detector equilibration are shown in orange.

559

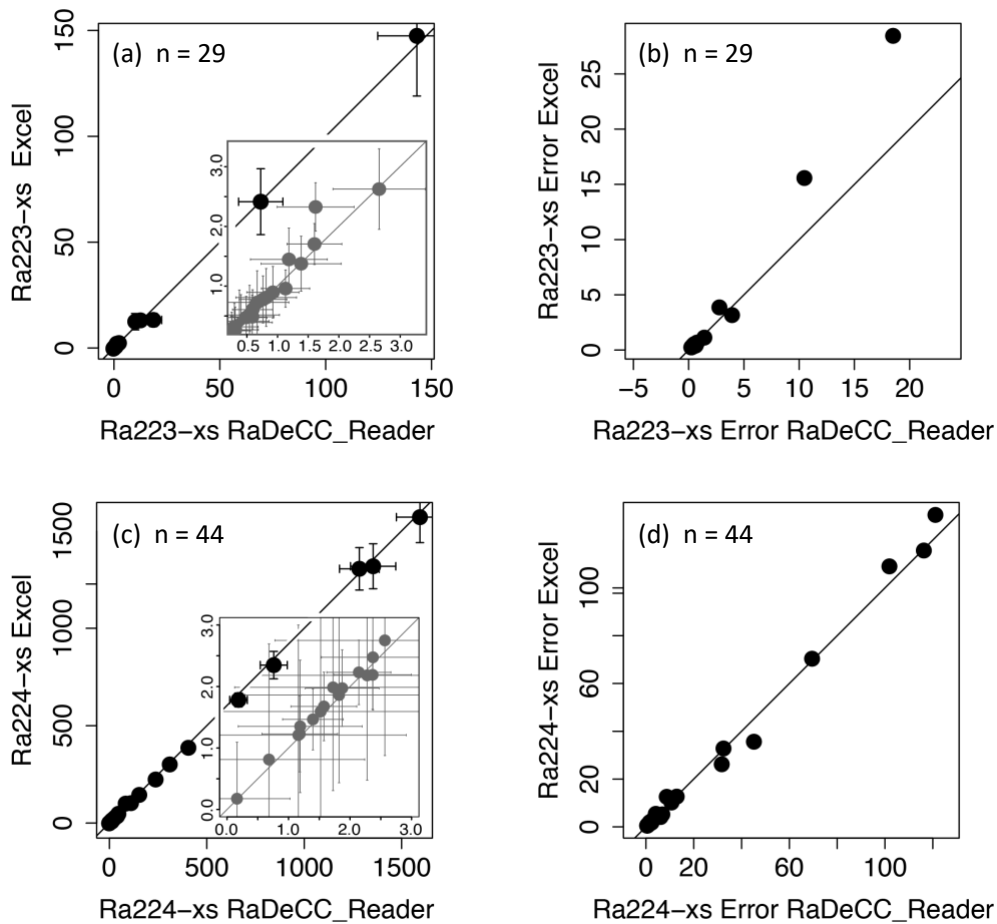


560

561 **Figure 4.** Flow charts of the guidelines for quantifying radium-223 (a) and radium-224 (b)

562 using RaDeCC apparatus (modified after Diego-Feliu et al. (2020). $CR_{220/219}$ is the count rate
563 ratio of the 220-channel to the 219-channel.

564



565

566 **Figure 5.** Validation of RaDeCC Reader outputs. Volume corrected activities and propagated

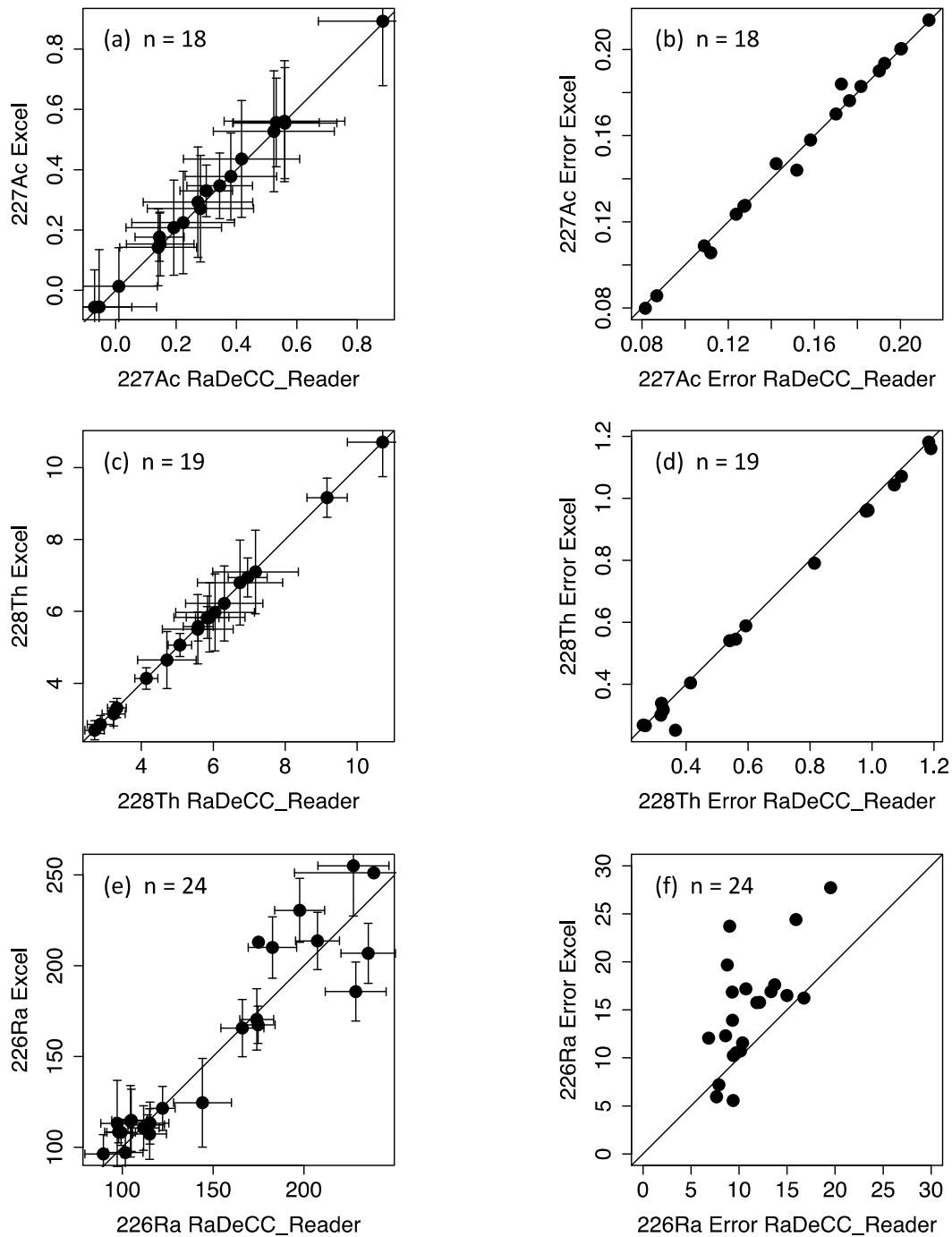
567 uncertainties of excess radium-223 (a, b) and excess radium-223 (c, d) determined by the

568 RaDeCC Reader program vs. an Excel implementation. Individual reads are plotted as black

569 circles in units of dpm/m^3 , relative to a 1:1 line. Inset plots (a, c) show the agreement between

570 RaDeCC Reader program and the Excel implementation for samples in the low activity

571 range.



572

573 **Figure 6.** Volume corrected activities (dpm/m^3) of actinium-227 (a), thorium-228 (c) and
 574 radium-226 (e). Propagated uncertainties associated with the calculation of actinium-227 (b),
 575 thorium-228 (d) and radium-226 are also included. Individual samples are plotted as black
 576 circles in units of dpm/m^3 , relative to a 1:1 line.

577

578 **Table 1.** Glossary of variable terms used, their descriptions and units.

Variable	Description	Units
<i>Y 219 CC</i>	Erroneously registered 219 channel chance coincidence counts	cpm
<i>Y 220 CC</i>	Erroneously registered 220 channel chance coincidence counts	cpm
<i>cpm219</i>	counts per minute (219 channel)	cpm
<i>cpm220</i>	counts per minute (220 channel)	cpm
<i>cpm total</i>	counts per minute (total channel)	cpm
<i>corr219</i>	cpm219 corrected for Y 219 CC	cpm
<i>corr220</i>	cpm219 corrected for Y 220 CC	cpm
<i>final219</i>	corr219 corrected for cross-channel interference	cpm
<i>final220</i>	corr219 corrected for cross-channel interference	cpm
<i>E219</i>	Detection efficiency of the 219 channel	-
<i>E220</i>	Detection efficiency of the 220 channel	-
<i>Ratio_{219/220}</i>	Detection efficiency ratio of the 219 and 220 channels	-
<i>P₂₁₉</i>	Probability of radon-219 decaying in the cell	-
<i>P₂₂₀</i>	Probability of radon-220 decaying in the cell	-
<i>L₂₁₉</i>	Loss resulting from the 219 channel delay and window settings	-
<i>L₂₂₀</i>	Loss resulting from the 220 channel delay and window settings	-
<i>bkgcorr223</i>	final219 corrected for background	cpm
<i>bkgcorr224</i>	final220 corrected for background	cpm
<i>dpm223</i>	final219 corrected for detection efficiency	dpm
<i>dpm224</i>	final220 corrected for detection efficiency	dpm
<i>vdpm223</i>	dpm223 corrected for sample volume	dpm m ⁻³
<i>vdpm224</i>	dpm224 corrected for sample volume	dpm m ⁻³
<i>²²³Ra_i</i>	vdpm223 for the initial read (including supported fraction)	dpm m ⁻³
<i>²²³Ra_s</i>	vdpm223 for the latter read (supported fraction only)	dpm m ⁻³
<i>²²⁴Ra_i</i>	vdpm224 for the initial read (including supported fraction)	dpm m ⁻³
<i>²²⁴Ra_s</i>	vdpm224 for the latter read (supported fraction only)	dpm m ⁻³
<i>λ₂₂₃</i>	Decay constant for radium-223	d ⁻¹
<i>λ₂₂₄</i>	Decay constant for radium-224	d ⁻¹
<i>²²³Ra_{xs}</i>	Excess radium-223 activity	dpm m ⁻³
<i>²²⁴Ra_{xs}</i>	Excess radium-224 activity	dpm m ⁻³
<i>vdpm226</i>	radium-226 activity	dpm m ⁻³
<i>vdpm226_{initial}</i>	radium-226 activity initially measured in sample	cpm m ⁻³
<i>slope of cpm total</i>	Gradient of counts over time in the total channel	cpm min ⁻¹
<i>m</i>	Radium-226 conversion factor	min ⁻¹
<i>E226</i>	Detection efficiency for radium-226	-
<i>Volume</i>	Volume or mass of sample water	L, kg